

Wire-on-Wire Growth of Fluorescent Organic Heterojunctions

Jian Yao Zheng,^{†,§} Yongli Yan,^{†,§} Xiaopeng Wang,[†] Yong Sheng Zhao,^{*,†} Jiaying Huang,[‡] and Jiannian Yao^{*,†}

[†]Beijing National Laboratory for Molecular Sciences (BNLMS), Key Laboratory of Photochemistry, Institute of Chemistry, Chinese Academy of Sciences, Beijing 100190, China

[‡]Department of Materials Science and Engineering, Northwestern University, Evanston, Illinois 60208-3108, United States

S Supporting Information

ABSTRACT: Dendritic organic heterojunctions with aluminum tris(8-hydroxyquinoline) (Alq₃) microwire trunks and 1,5-diaminoanthraquinone (DAAQ) nanowire branches were prepared by a two-step growth process. The prefabricated Alq₃ microwires act as nucleation centers for site-specific secondary vapor growth of DAAQ nanowires, resulting in the unique dendritic heterostructures. When the trunk was excited with a focused laser beam, emitted light of various colors was simultaneously channeled from the branched nanowires via both waveguiding and energy transfer. The intensity of the out-coupled emissions was modulated effectively by changing the polarization of the incident light.

One-dimensional (1D) nanomaterials, especially nanowires, are ultimately suitable for the transport of photons, electrons, and excitons and have been demonstrated as building blocks of optical circuits.^{1–4} Assembling nanowires into complex heterostructures with high spatial and angular precision is critical for realizing functional devices, including photonic routers,⁵ modulators, and polarization rotators.⁶ Techniques such as micromanipulation⁷ and single-beam optical traps⁸ have been developed to manipulate and assemble individual nanowires into heterojunctions. An alternative method is to create nanowire heterojunctions (NWHJs) via direct epitaxial growth. For example, several inorganic NWHJs have successfully been obtained by dendritic crystal growth and subsequently incorporated into nanoscale photonic devices.^{9–13}

The direct growth of organic NWHJs has not been extensively investigated to date, although organic nanomaterials have been shown to have new photonic and electronic properties.^{14,15} The optical properties of organic nanomaterials could be effectively tailored through rational molecular design, and the intermolecular energy transfers between components with matching energy levels could lead to new optical properties unique to organic NWHJs.¹⁶ For example, the exciton polaritons formed by the strong coupling between photons and Frenkel excitons in organic nanowires can significantly increase the refractive index.^{17–20} This can help to break the diffraction limit when the dimensions of the nanowire optical components are reduced to the subwavelength scale, which is beneficial to the further miniaturization of optical devices. In this paper, we report a two-step synthesis of organic NWHJs composed of aluminum tris(8-hydroxyquinoline)

(Alq₃) trunks and 1,5-diaminoanthraquinone (DAAQ) branches. The preformed Alq₃ microwires, made by self-assembly in the liquid phase, were used as nucleation centers for the site-specific secondary epitaxial vapor growth of DAAQ branches to give dendritic heterostructures with optical channeling properties. When the Alq₃ trunk was excited with a focused laser, light emission of various colors could be out-coupled from the branches via optical waveguiding and energy transfer. The intensity of the out-coupled light varied sinusoidally when the polarization angle of the incident laser was rotated in a circle around the long axis of the Alq₃ trunk. NWHJ-based optical channels should hold promise for the construction of various types of multiplexer and circuit components in future applications.²¹

In our earlier work, it was found that during physical vapor deposition, the vaporized organic molecules tend to nucleate preferentially and grow more rapidly on sites with smaller curvature radii and higher surface energies, such as dusts, particles, and metal needles.^{22,23} Inspired by these results, here we extended the work further to create dendritic organic wire-on-wire heterojunctions by a two-step growth process in which preformed organic microwires are used as seeds for the growth of vertically aligned organic nanowires of a second compound. In this work, we chose as model compounds Alq₃ and DAAQ (Figure S1 in the Supporting Information), two organic dyes that are widely used in organic optoelectronic devices. The absorption spectrum of DAAQ overlaps well with the photoluminescence (PL) spectrum of Alq₃ (Figure S2), ensuring efficient energy transfer between the two compounds in the heterostructures. The NWHJs were prepared by a two-step method (Figure 1A). First, ultralong single-crystal Alq₃ microwires with hexagonal cross sections (Figure 1B) were prepared using an antisolvent diffusion method combined with solvent-evaporation-induced self-assembly (Figure S3).²⁴ The wafers with Alq₃ microwires were subsequently used as substrates for the secondary growth of DAAQ by physical vapor deposition (Figure S4). During the deposition, the vaporized DAAQ selectively nucleated and grew perpendicularly on the surfaces of the Alq₃ wires to form NWHJs.

In the first step, the growth of the Alq₃ microwires can be finely controlled since the slow evaporation of the antisolvent ensures a proper degree of saturation of the solution.²⁴ Figure S5 reveals the time-dependent morphology evolution of the

Received: November 2, 2011

Published: January 30, 2012

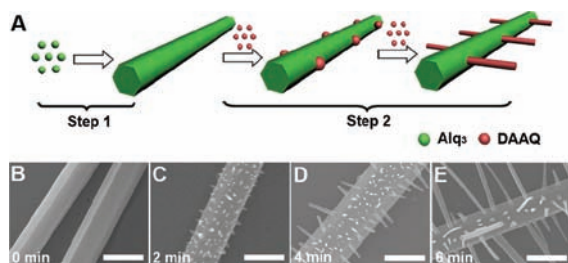


Figure 1. Schematic illustration and corresponding SEM images showing the growth process of the dendritic organic NWHJs. (A) Step 1: Alq₃ microwires are made by liquid-phase self-assembly. Step 2: Site-specific nucleation and epitaxial growth of vertical DAAQ nanowires on the surfaces of Alq₃ by physical vapor deposition. (B–E) SEM images of (B) Alq₃ microwires formed in step 1 and (C–E) different stages of DAAQ growth in step 2. DAAQ first nucleates on the Alq₃ wire surfaces to form some isolated clusters, seeding subsequent molecular deposition to form the final vertical nanowire branches. All scale bars are 2 μm .

Alq₃ crystals. First, the Alq₃ molecules aggregated to form small particles with the initial solvent evaporation. The vapor pressure of the antisolvent allowed a continuous dissolution equilibrium for the particles, enabling them to grow and recrystallize step-by-step to form 1D microstructures. When the assembly process continued for over 10 h, single-crystalline microwires with hexagonal cross sections and smooth surfaces (Figure 1B), which are favorable for optical waveguiding purposes, were finally obtained.

Alq₃ microwires dispersed onto silicon and quartz wafers were used as the substrates for the epitaxial vapor growth of DAAQ. Figure 1 and Figure S6 show that DAAQ selectively nucleated and grew on the surfaces of the Alq₃ wires, especially at the arrises of the hexagonal prisms, and almost no DAAQ products were obtained on the smooth wafer areas. The Alq₃ microwires played the role of condensation nuclei to help the precipitation, similar to the role of AgI in artificial rain. As illustrated in Figure 1A,C, the small curvature radii and organic nature of Alq₃ make the microwires the preferential sites for condensation of the DAAQ vapor over the smooth surface of Si wafers. DAAQ first nucleated on the Alq₃ wire surfaces to form some isolated clusters at the initial stage of the deposition. In the following stage, the vapor diffusion was much faster than the self-nucleation of DAAQ clusters. In addition, the surface energies determined that the [100] length direction should increase much faster than the diameter dimensions, which is a favorable condition for the growth of long wires.²⁵ According to the growth process, the length and positioning density of the DAAQ branches could be modulated by changing the growth time (Figure 1C). As shown in Figure S6, we were also able to achieve precise control of the growth density of DAAQ wires with fixed lengths by tuning the growth temperature.

Figure 2A,B shows typical scanning electron microscopy (SEM) images of Alq₃–DAAQ NWHJs prepared by growing the DAAQ branches at 185 °C for 6 min. The average length and diameter of the DAAQ branches are 5 μm and 350 nm, respectively. The interface between the DAAQ nanowires and the Alq₃ trunks is sharp and can be clearly identified. The transmission electron microscopy (TEM) images and selected-area electron diffraction (SAED) patterns of the NWHJs in Figure 2C show the diffraction patterns of Alq₃ and DAAQ from the trunk and the branches, respectively. The branches grew perpendicularly to the trunks. The SAED patterns (Figure

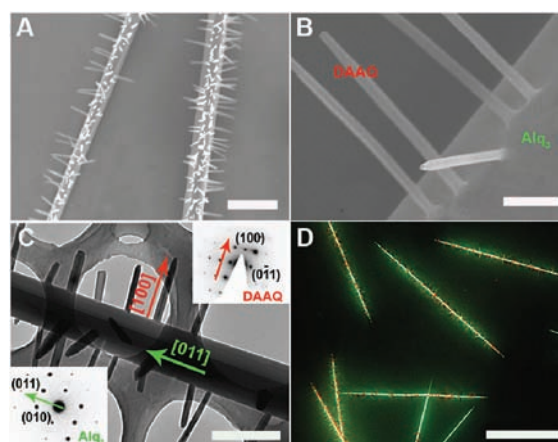


Figure 2. Characterization of the organic heterojunctions. (A, B) SEM images of the Alq₃–DAAQ dendritic heterostructures. Scale bars: (A) 5 μm ; (B) 1 μm . (C) TEM image of a single NWHJ. Scale bar is 5 μm . Insets: SAED patterns of the Alq₃ trunk and DAAQ branch. The Alq₃ and DAAQ have single-crystal structures; Alq₃ grew in the [011] direction, while [100] was the preferential growth direction for the branch component of DAAQ. (D) PL microscopy images of the NWHJs excited with the UV band (330–380 nm) of a mercury lamp. Scale bar is 100 μm . The green emission is from the Alq₃ trunks and the red emission from the DAAQ branches.

2C insets) also indicate that both the trunks and branches were single-crystalline, growing along their [011] and [100] directions, respectively. Energy dispersive X-ray spectroscopy (EDS) analysis (Figure S7) further testified that the chemical compositions of the trunks and branches were Alq₃ and DAAQ, respectively. In the PL microscopy images taken under UV excitation (Figure 2D), the dendritic structures appear to have green-emitting trunks and red-emitting branches, consistent with the PL spectra of the two components (Figure S2).

This unique dendritic heterostructures exhibit optical channeling properties.^{5,26} The schematic illustration in Figure 3A shows the concept of the optical channels from such NWHJs. When the trunk is excited with an input laser signal, the emitted green light propagates toward its distal ends. The green light is out-coupled to the branches via two processes: The first is Förster resonance energy transfer (FRET), whereby the red PL of DAAQ is excited at the interfaces of the junctions. The second is photon reabsorption, in which the Alq₃ emission guided in the microwire may be scattered at the junctions and injected into the DAAQ nanowires, causing absorbance along the nanowire cavities. As a result, the PL of Alq₃ is partially quenched, and the green and red emissions are guided toward the tips of the branches. Therefore, different color signals are output from each branch depending on the relative fraction of the two types of emissions as the propagation length increases. Figure 3B shows a single typical NWHJ used for the photonic characterizations, which consisted of more than 100 DAAQ branches grown on a single Alq₃ trunk with an average spacing of ~ 1 μm . Both the trunk and branches exhibited typical characteristics of active optical waveguides with bright luminescence emission at the tips. The guided light could indeed be output simultaneously from the tips of the trunks and different branches when the middle area of the Alq₃ wire was excited with a 351 nm focused laser beam (Figure 3C).

The spatially resolved PL spectra in Figure 3D demonstrate the propagation-length-dependent out-coupling emission. The spectrum taken locally from the excited spot shows the typical

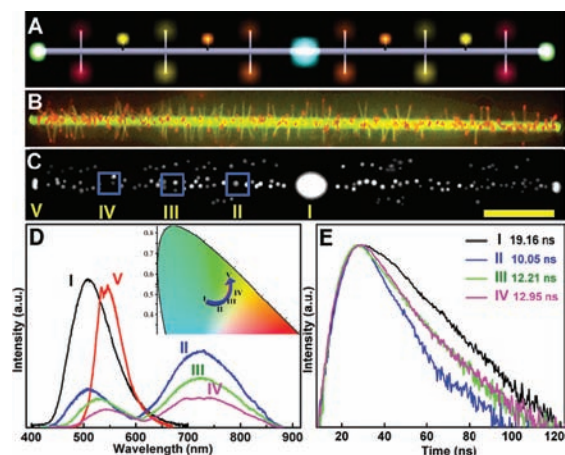


Figure 3. Optical routing via the organic NWHJs. (A) Schematic illustration of the Alq₃-DAAQ NWHJ-based optical routers. A UV laser beam is focused on the Alq₃ microwire to excite its fluorescence, which propagates along the trunk and channels to the DAAQ branches. (B) PL microscopy image of a single NWHJ excited with the UV band of a mercury lamp. (C) PL image of the NWHJ in (B) excited with a 351 nm focused laser beam, demonstrating the optical channeling illustrated in (A). The blue boxes indicate the areas selected for collection of spectra. The scale bar is 25 μm . (D) PL spectra of the excited spot (I) and the output signals from the DAAQ branches (II–IV) and the Alq₃ tip (V) taken from the regions marked in C. The inset shows the variation of the CIE coordinates with the propagation length. (E) PL decay profiles of the 515 nm Alq₃ emissions indicating the variation of the energy transfer efficiencies from Alq₃ to DAAQ at different propagation lengths.

emission of Alq₃ in the 450–700 nm region. The emission can propagate efficiently along the trunk and couple to the branches. At the branch tips, the DAAQ red emission (600–850 nm) emerges at the expense of that from Alq₃. This indicates that an efficient FRET process took place at the interfaces of the junctions and photon reabsorption along the DAAQ nanowires occurred, resulting in the diffusion of the photogenerated excitons from Alq₃ to DAAQ.¹⁶ The out-coupled light from the branch tips is a superposition of the green and red emissions from the two compositions. It is noteworthy that the Alq₃ emission part showed an obvious red shift with increasing guided length because the shorter-wavelength portion was absorbed more efficiently by the DAAQ branches during propagation, as proved by the spectral overlap shown in Figure S2. The coupled light from the trunk tip is a red-shifted Alq₃ emission with some waveguided modes between 530 and 560 nm. The CIE coordinates of the coupled light calculated from the PL spectra (Figure 3D inset) clearly showed variations of the output signals.

The PL decay behavior was measured to study the photon and exciton interactions between the trunk and the branches. Figure 3E depicts the PL decay profiles taken from the different positions marked in Figure 3C monitored with the Alq₃ emission at 515 nm. The PL lifetime at the excited spot (τ_0) was 19.16 ns, revealing the intrinsic exciton lifetime of Alq₃ without extrinsic PL quenching.²⁷ At the output channels, the lifetime (τ_m) was decreased to 10.05, 12.21, and 12.95 ns, respectively in the presence of the DAAQ energy acceptor.¹⁶ The energy transfer efficiencies (η_m) at different channels were calculated using the equation $\eta_m = 1 - \tau_m/\tau_0$, which gave efficiencies of 47.5, 36.3, and 32.4% at II, III, and IV, respectively. The efficiency decreased with increasing prop-

agation length because the red shift of the Alq₃ emission decreased the spectral overlap integral as shown in Figure S2, resulting in the fluctuation of the green and red emissions.

The dendritic structure offers a model system for demonstrating that the output from the nanowire channels can be actively controlled by modulating the input. The fast-developing optical technology provides a solution to the bandwidth and capacity limitations that the modern computing industry is approaching.^{6,28} The photon is a fundamental carrier of information, possessing numerous information-carrying degrees of freedom (frequency, phase, polarization, etc.). In this work, polarization, one of the most essential properties of light, was adopted to modulate the color and intensity of the output signals from the branch channels simultaneously. The optical measurements were carried out with a home-built optical microscope system (Figure S8). Figure 4A schematically

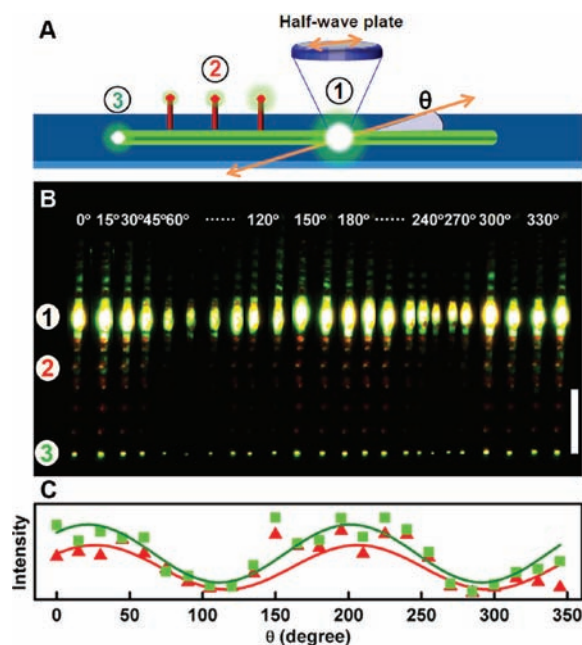


Figure 4. Modulation of the output intensity by variation of the incident polarization angle. (A) Schematic illustration of the experimental setup for polarized excitation. θ is the angle between the incident light polarization and the long axis of the Alq₃ wire. A single NWHJ was excited with a linearly polarized laser beam at input 1, and the modulated light signals were collected at two different output channels 2 and 3. (B) PL images of the NWHJ taken by exciting the middle area 1 at different polarization angles ($\theta = 0^\circ$ – 360°). Light channeling from the trunk to the wire branches can be clearly observed. The emission intensity varied in an oscillatory manner between maximum and minimum values. The vertical scale bar is 20 μm . (C) Polarization-angle-dependent PL intensity measured from the branch channel 2 (red, 720 nm) and the trunk channel 3 (green, 542 nm). The highest PL intensities of these two outputs were observed at $\theta = 15^\circ$. The PL intensity decreased gradually with increasing θ and reached its minimum at $\theta = 105^\circ$, indicating a sinusoidally modulated out-coupling with a period of 180° .

shows a typical experiment in which a single NWHJ was excited with a linearly polarized laser beam. The parameter θ refers to the angle between the long axis of the Alq₃ wire and the incident polarization, which was adjusted using a half-wave plate. Light channeling from the trunk to the wire branches was clearly observed. The emission intensity varied in an oscillatory manner between a maximum and minimum value (Figure 4B),

implying a strong polarization dependence of the in-coupling efficiency. Figure 4C shows the emission intensities from wire ends 2 and 3 as functions of θ . It indicates that the highest PL intensities of these two outputs were observed at $\theta = 15^\circ$, giving an insight into the preferred direction of the π -conjugated alignment in the Alq₃ crystalline trunk. The PL intensity decreased gradually with increasing θ and reached its minimum at $\theta = 105^\circ$, indicating a sinusoidally modulated out-coupling with a period of 180° .

It was observed that the light emission could be varied from a maximally emitting "on" state to a minimally emitting "off" state. The on/off ratio $R = I_{\max}/I_{\min}$ (where I_{\max} and I_{\min} represent the intensities of the light polarized parallel and perpendicular to the transition dipole moment, respectively) was determined to be as large as 6.7. For a quantitative analysis of the modulation of the output emission, a parameter ρ called the polarization ratio was defined as $\rho = (R - 1)/(R + 1)$.²⁹ Here, $\rho = 0.74$ was obtained for the output of the branch channels. This ratio is larger than those of the previously reported conjugated polymer nanowires ($\rho = 0.6$)³⁰ and inorganic semiconductor CdSe nanowires ($\rho \approx 0.6$).³¹ In this way, propagating light in the NWHJs can be specifically modulated by controlling the incident polarization. We believe this concept can be further generalized and expanded to more complex structures that can combine several kinds of optical signals simultaneously. A multiple-input, multiple-output optical channel might serve as an efficient splitter, switcher, and/or multiplexer in future photonic networks designed for computing and information processing.

In conclusion, we have reported a two-step wire-on-wire approach for the synthesis of branched nanowire heterostructures of two organic materials. Site-specific nucleation and epitaxial growth of DAAQ on the prefabricated Alq₃ microwires can be controlled to form dendritic heterostructures with desired spatial positioning. Simultaneous coupling of the photogenerated excitons from the trunk to the branches via waveguiding and energy transfer lead to optical channeling with multiple outputs, which may be useful for optical routers in miniaturized photonic circuits. The output intensity from the wire channels varied sinusoidally upon rotation of the incident polarization. Such controllable optical channels and routers may find numerous applications in nanoscale optical devices, circuits, and networks.

■ ASSOCIATED CONTENT

● Supporting Information

Experimental details; molecular structures and absorption and PL spectra of Alq₃ and DAAQ; schematic illustrations of the preparation of the Alq₃ microwires and the physical vapor deposition setup for the growth of DAAQ nanowire branches; time-dependent morphology evolution of the Alq₃ crystals; SEM images of the heterojunctions obtained at different growth temperatures of DAAQ; EDS analysis of a single Alq₃-DAAQ NWHJ; and schematic demonstration of the experimental setup for the optical characterization. This material is available free of charge via the Internet at <http://pubs.acs.org>.

■ AUTHOR INFORMATION

Corresponding Author

yszhaoy@iccas.ac.cn; jnyao@iccas.ac.cn

Author Contributions

[§]These authors contributed equally.

■ ACKNOWLEDGMENTS

Mr. Jianming Chen is gratefully acknowledged for his helpful discussions. This work was supported by the National Natural Science Foundation of China (21125315, 91022022, and 51073164), the Chinese Academy of Sciences, and the National Basic Research Program (973 Program) of China. J.H. thanks the Alfred P. Sloan Foundation for a Research Fellowship.

■ REFERENCES

- (1) Almeida, V. R.; Barrios, C. A.; Panepucci, R. R.; Lipson, M. *Nature* **2004**, *431*, 1081.
- (2) Yu, G.; Lieber, C. M. *Pure Appl. Chem.* **2010**, *82*, 2295.
- (3) Yan, H.; Choe, H. S.; Nam, S.; Hu, Y.; Das, S.; Klemic, J. F.; Ellenbogen, J. C.; Lieber, C. M. *Nature* **2011**, *470*, 240.
- (4) Yan, R. X.; Gargas, D.; Yang, P. D. *Nat. Photonics* **2009**, *3*, 569.
- (5) Sirbuly, D. J.; Law, M.; Pauzauskie, P.; Yan, H.; Maslov, A. V.; Knutsen, K.; Ning, C.-Z.; Saykally, R. J.; Yang, P. *Proc. Natl. Acad. Sci. U.S.A.* **2005**, *102*, 7800.
- (6) Wei, H.; Wang, Z.; Tian, X.; Kall, M.; Xu, H. *Nat. Commun.* **2011**, *2*, 387.
- (7) Law, M.; Sirbuly, D. J.; Johnson, J. C.; Goldberger, J.; Saykally, R. J.; Yang, P. D. *Science* **2004**, *305*, 1269.
- (8) Agarwal, R.; Ladavac, K.; Roichman, Y.; Yu, G. H.; Lieber, C. M.; Grier, D. G. *Opt. Express* **2005**, *13*, 8906.
- (9) Jiang, X.; Tian, B.; Xiang, J.; Qian, F.; Zheng, G.; Wang, H.; Mai, L.; Lieber, C. M. *Proc. Natl. Acad. Sci. U.S.A.* **2011**, *108*, 12212.
- (10) Yan, H.; He, R.; Johnson, J.; Law, M.; Saykally, R. J.; Yang, P. J. *Am. Chem. Soc.* **2003**, *125*, 4728.
- (11) Jung, Y.; Ko, D.-K.; Agarwal, R. *Nano Lett.* **2006**, *7*, 264.
- (12) Zhu, J.; Peng, H.; Marshall, A. F.; Barnett, D. M.; Nix, W. D.; Cui, Y. *Nat. Nanotechnol.* **2008**, *3*, 477.
- (13) Bierman, M. J.; Lau, Y. K.; Kvit, A. V.; Schmitt, A. L.; Jin, S. *Science* **2008**, *320*, 1060.
- (14) Zang, L.; Che, Y. K.; Moore, J. S. *Acc. Chem. Res.* **2008**, *41*, 1596.
- (15) Zhao, Y. S.; Fu, H. B.; Peng, A. D.; Ma, Y.; Liao, Q.; Yao, J. N. *Acc. Chem. Res.* **2010**, *43*, 409.
- (16) Zhao, Y. S.; Fu, H. B.; Hu, F. Q.; Peng, A. D.; Yang, W. S.; Yao, J. N. *Adv. Mater.* **2008**, *20*, 79.
- (17) Takazawa, K.; Inoue, J.-i.; Mitsuishi, K.; Takamasu, T. *Phys. Rev. Lett.* **2010**, *105*, No. 067401.
- (18) Zhang, C.; Zheng, J. Y.; Zhao, Y. S.; Yao, J. *Adv. Mater.* **2011**, *23*, 1380.
- (19) Takazawa, K.; Inoue, J.-i.; Mitsuishi, K.; Takamasu, T. *Adv. Mater.* **2011**, *23*, 3659.
- (20) Zhang, C.; Zou, C.-L.; Yan, Y.; Hao, R.; Sun, F.-W.; Han, Z.-F.; Zhao, Y. S.; Yao, J. *J. Am. Chem. Soc.* **2011**, *133*, 7276.
- (21) Tucker, R. S. *Nat. Photonics* **2010**, *4*, 405.
- (22) Zhao, Y. S.; Wu, J. S.; Huang, J. X. *J. Am. Chem. Soc.* **2009**, *131*, 3158.
- (23) Zhao, Y. S.; Zhan, P.; Kim, J.; Sun, C.; Huang, J. X. *ACS Nano* **2010**, *4*, 1630.
- (24) Xu, G.; Tang, Y.-B.; Tsang, C.-H.; Zapien, J.-A.; Lee, C.-S.; Wong, N.-B. *J. Mater. Chem.* **2010**, *20*, 3006.
- (25) Dick, K. A.; Deppert, K.; Larsson, M. W.; Martensson, T.; Seifert, W.; Wallenberg, L. R.; Samuelson, L. *Nat. Mater.* **2004**, *3*, 380.
- (26) Fang, Y. R.; Li, Z. P.; Huang, Y. Z.; Zhang, S. P.; Nordlander, P.; Halas, N. J.; Xu, H. X. *Nano Lett.* **2010**, *10*, 1950.
- (27) Tang, C. W.; Vanslyke, S. A.; Chen, C. H. *J. Appl. Phys.* **1989**, *65*, 3610.
- (28) Caulfield, H. J.; Dolev, S. *Nat. Photonics* **2010**, *4*, 261.
- (29) Bao, Q. L.; Goh, B. M.; Yan, B.; Yu, T.; Shen, Z. A.; Loh, K. P. *Adv. Mater.* **2010**, *22*, 3661.
- (30) Moynihan, S.; Lovera, P.; O'Carroll, D.; Iacopino, D.; Redmond, G. *Adv. Mater.* **2008**, *20*, 2497.
- (31) Shan, C. X.; Liu, Z.; Hark, S. K. *Phys. Rev. B* **2006**, *74*, No. 153402.